



Differential microphone array: Design for acoustic localization within aircraft cabins

Benoît Meriot, Jérémie Derré, Olivier Bareille, Mohamed Ichchou, Daniel Juvé

► To cite this version:

Benoît Meriot, Jérémie Derré, Olivier Bareille, Mohamed Ichchou, Daniel Juvé. Differential microphone array: Design for acoustic localization within aircraft cabins. 26th International Congress on Sound and Vibration, ICSV 2019, Jul 2019, Montreal, Canada. <hal-03851967>

HAL Id: hal-03851967

<https://hal.science/hal-03851967v1>

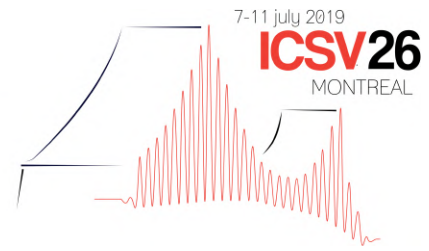
Submitted on 31 Oct 2024

HAL is a multi-disciplinary open access archive for the deposit and dissemination of scientific research documents, whether they are published or not. The documents may come from teaching and research institutions in France or abroad, or from public or private research centers.

L'archive ouverte pluridisciplinaire **HAL**, est destinée au dépôt et à la diffusion de documents scientifiques de niveau recherche, publiés ou non, émanant des établissements d'enseignement et de recherche français ou étrangers, des laboratoires publics ou privés.



Distributed under a Creative Commons CC BY 4.0 - Attribution - International License



DIFFERENTIAL MICROPHONE ARRAY: DESIGN FOR ACOUSTIC LOCALIZATION WITHIN AIRCRAFT CABINS

Benoît Meriot, Jérémie Derré

Airbus Operations SAS

email: benoit.meriot@airbus.com

Olivier Bareille *, Mohamed Ichchou *, and Daniel Juvé

*Ecole Centrale de Lyon, LTDS UMR CNRS 5513 *, LMFA UMR CNRS 5509*

This paper presents the modeling, numerical simulations and experimental results of a differential microphone array and its associated post-processing methods. This study combines the development of an array geometry and the definition of a post-processing method adapted to applications within an aircraft. The research originality lies in the considered array and post-processing method, based on the approximation of the pressure gradient by a differential microphone calculation and linear combination of the signals. As the targeted frequency range of interest is from 200 Hz up to 5000 Hz, a fourth-order linear array is chosen, in order to handle at the same time the space constraints due to the aircraft environment and the inter-microphone spacing linked to the frequency range. The frequency band target is used to drive the antenna geometry definition. An experimental proof of concept is tested in an anechoic room. Simulations and experimental results are compared to an analytical model. The comparison highlights the method advantages as well as the experimental limitations of the designed linear array. Then, a first localization test is performed and finally, a modification of the post-processing method is suggested, to improve the directivity of the array low frequency.

Keywords: differential microphone array, noise localization, aircraft, cabin noise

1. Introduction

The air traffic passenger number has been increasingly growing these last years, and associated with that, the global aircraft fleet. Therefore, aircraft manufacturers increase their delivery rates in order to respect their commitments, mature their products and stay innovative. In a production cycle, each aircraft follow systematic testings, including ground and flight configurations. While tested, some unexpected noises could appear. Most of the time, they are only the consequence of a defect : for instance, a whistling heard during cruise close to a door could be the sign of an airleak in the door perimeter. In more complex situations, the noise could not be easily identified with a single microphone. Therefore, acoustic localization array appears as an effective tool to characterize the acoustic field of aircraft interiors. Most of the arrays and methods used today are based on beamforming or acoustic holography. These methods are efficient but require large microphone arrays for applications to low- and mid-frequency range, which is thus complicated in aircraft interior, especially in the case of small reflective spaces such as the avionics

bay. Unlike beamforming applications and derivations, for which a great amount of information exists in the scientific literature, differential microphone arrays have not been extensively studied in the past and are still a subject of research for the community. Recent publications suggesting various uses of differential microphone arrays are briefly presented below.

In his book, Benesty [1] introduces the theory of differential microphone arrays. The model presented in this paper is based on the concepts presented in this work. In this paper discussions regarding the obtained results are made with regards to the theory and limitations introduced by Benesty.

Recently, Ducourneau [2] has suggested to use a differential microphone array to perform measurements of acoustic reflection coefficient in an industrial environment. Indeed, the directivity that can theoretically be achieved with a differential array makes the use of this post-processing method very interesting in such a context. In his work, Ducourneau shows how a super-directive linear array was built and characterized. The present paper suggests the use of the same kind of linear array, with a customized weighting adapted to our needs of sound source localization within an aircraft.

Other works have already suggested the use of differential microphone arrays in a context of sound source localization. Huang [3] for instance, presents a circular differential array capable of electronic steering. In this paper, the focus is put on the design of a linear array aimed at being used in a distributed network of arrays.

2. Model

This section presents the array and signal processing modeling. First, the general principle is described, with the associated limitations. Then the array construction principle is proposed, with a focus on the fourth-order array that has been selected for this study. Finally, the obtained directivity is sketched in an angular plot.

2.1 Principle

The microphone array developed in this study is based on the concept of differential microphone arrays of high order. This principle allows to create an array of order n , whose response is proportional to a linear combination of the acoustic pressure spatial derivatives up to the n^{th} order. The principle of finite differences is used to obtain this sensitivity to the pressure spatial derivatives, resulting in the directivity of the array. Considering the propagation of a acoustic plane wave, the pressure field can be expressed as the equation 1

$$p(k, \mathbf{r}, t) = P_0 e^{j(\omega t - \mathbf{k} \cdot \mathbf{r} \cos \theta)}, \quad (1)$$

where P_0 is the plane wave amplitude, ω the angular frequency, T the matrix transposition operator, and $k = \frac{\omega}{c}$ the wave-number vector. θ is the incidence angle between \mathbf{r} and \mathbf{k} . Removing the temporal dependency, the n^{th} order derivative of the pressure field along the direction \mathbf{r} can be expressed as the equation 2

$$\frac{\partial^n p(k, r)}{\partial r^n} = P_0 (-jk \cos \theta)^n e^{jk r \cos \theta}. \quad (2)$$

This expression highlights the bidirectional directivity of an n^{th} order array, proportional to $(\cos \theta)^n$. Therefore being able to evaluate the n^{th} order derivative of the pressure field in a given direction \mathbf{r}_0 produces an array sensitive mainly to the waves propagating along that direction, and weights down with a factor $(\cos \theta)^n$ the waves propagating along directions \mathbf{k} differing from \mathbf{r}_0 .

2.2 Frequency range limitations

The targeted frequency range for the desired array is 200 Hz-5000 Hz. The theory of differential microphone arrays, as explained in [1], shows that an array with a microphone spacing of 2.5cm should allow to address this targeted frequency range. However, the assumption is based on the hypothesis of perfectly matched microphones. In the real world, this hypothesis is not valid and slight phases mismatch between microphones can lead to errors in the finite differences estimation of the pressure gradient, especially in the lower frequency range. This constraint leads us to an array composed of several sub-arrays, with inter-element spacing varying from 2.5 cm to 15 cm. The principle used here to create a super-directive array relies on the principle of cascading several "first order" microphone dipoles. The number of cascades being equal to the order of the array. This means if n is the number of microphones used, the array will have a maximum order of $n - 1$. Benesty [1], explains how a high order array is more sensitive to a phenomena called white noise gain (WNG) than an array of lower order. This is why a trade-off has to be made between narrow directivity produced by a high order array, with a high number microphones, and an array with fewer microphones, but with better performances at low frequencies. Hence, in a first step, sub-arrays based on 5 equally spaced microphones are chosen, resulting in a combined array of the fourth-order addressing the targeted frequency range.

2.3 First-order array

Let us consider in a first step two microphones and an acoustic plane wave arriving with an incidence angle θ and a pulsation ω . The response of this first-order array, resulting from the introduction of delay τ and a difference between the signal, can be expressed as the equation 3

$$E_1(\omega, \theta) = P_0 (1 - e^{-j\omega(\tau + \frac{d}{c} \cos \theta)}). \quad (3)$$

For $kd \ll \pi$ and $\omega\tau \ll \pi$, this response can be normalized and expressed as

$$E_{N_1}(\theta) = a_0 + a_1 \cos \theta = \alpha_1 + (1 - \alpha_1) \cos \theta, \quad (4)$$

with

$$\alpha_1 = a_0 = \frac{\tau}{\tau + d/c} = \frac{\tau}{\tau + \tau_0}, \quad (5)$$

and

$$1 - \alpha_1 = a_1 = \frac{d/c}{\tau + d/c} = \frac{d/c}{\tau + \tau_0}. \quad (6)$$

This expression highlights how α_1 drives the shape of the directivity of the first order array.

The response of the first order array can also be expressed in a matrix form, highlighting the relationship between the received signals and the array response through the applied weighting applied. This weighting \mathbf{h} is chosen according to the desired directivity shape. The array response \mathbf{S} can then be expressed as a function of the received signals \mathbf{d} with

$$\begin{cases} d^H(\omega, \alpha_1) h_1(\omega) = S_1(\omega) \\ d^H(\omega, \alpha_2) h_1(\omega) = S_2(\omega) \end{cases} \quad (7)$$

With $\alpha_i = \cos(\theta_i)$ are the directions where we choose the array response S_1 and S_2 . We generally chose $S_1 = 1$ and $S_2 = 0$ to drive the directivity of the array. Then the weighting factor \mathbf{h} can be expressed as

$$\mathbf{h}(\omega) = \begin{bmatrix} h_1 \\ h_2 \end{bmatrix} = \frac{1}{1 - e^{-j\omega\tau_0(\alpha_2 - 1)}} \begin{bmatrix} 1 \\ -e^{-j\omega\tau_0\alpha_2} \end{bmatrix} \quad (8)$$

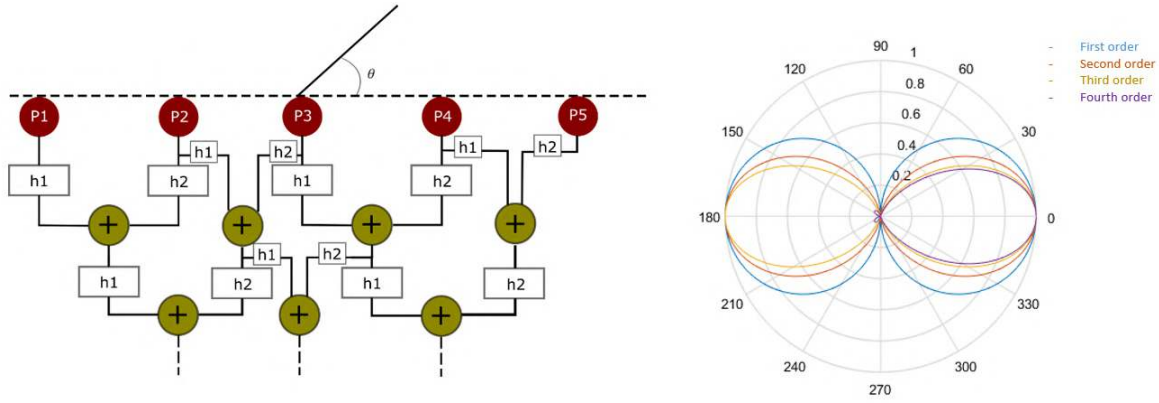


Figure 1: Combination of first-order sub-arrays responses and associated directivities.

2.4 Cascading a fourth-order array

A fourth-order array can be constructed by combining four first-order arrays. The response of the resulting array can be expressed as the product of the first order arrays' responses, such as

$$E_4(\omega, \theta) = P_0 \omega^4 \prod_{i=1}^4 [\alpha_i + (1 - \alpha_i) \cos \theta] . \quad (9)$$

The cascading principle, showing how the combination of first-order responses is performed and the effect on the resulting directivity is illustrated on figure 1. The first three stages of the cascading post-processing are performed using a weighting with $\theta_1 = 0$, $\theta_2 = 90^\circ$, $S_1 = 1$ and $S_2 = 0$. These stages allow to narrow the resulting directivity. The weighting of the fourth stage of the cascading is performed using $\theta_1 = 0$, $\theta_2 = 180^\circ$, $S_1 = 1$ and $S_2 = 0$. This last stage uses the weighting of a cardioid directivity, to create an array sensitive only to sound waves propagating from in the forward direction, and not from the opposite direction (180°). The obtained directivity at each stage of the cascading is illustrated on the figure 1.

3. Experimental set-up

As seen in the previous parts, for a given array orientation, choosing a direction θ_1 of focus of the array drives the directivity pattern. By comparison to the classical beamforming method, it is hence not possible to electronically steer differential arrays. That is why the experimental set-up described hereafter has been used.

In order to validate the model and the associated numerical simulations, an experimental campaign has been realized within an anechoic chamber, in Airbus Toulouse, as seen on figure 2. An omnidirectional noise source (Brüel&Kjær 4295) is used, driven by a wide band random signal. As during the tests the room was in a semi-anechoic configuration, with a hard reflecting floor, it has been decided to put the source radiating directly from the floor, in order to minimize the interaction between direct and reflected sound waves. A linear array of thirteen quarter-inch pressure-field microphones is mounted on a rotating boom over the source. The minimal distance between the closest sensor in vertical position (taken as the zero degree reference) is approximately 1 meter. The measurements have been realized with an angular increment of 5 degrees, leading to 72 measured positions. As it can be seen on figure 2, the metallic structure has been protected with foam, in order to reduce the diffraction and reflection effects. The

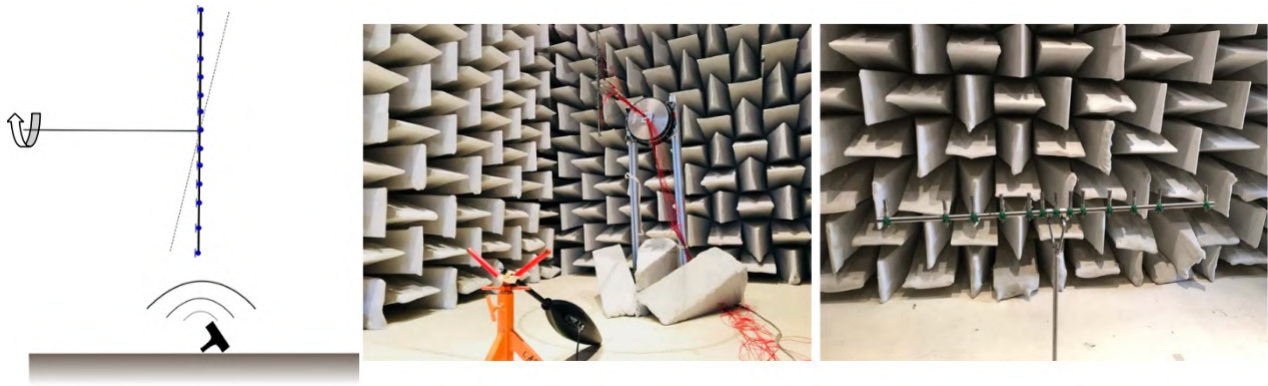


Figure 2: Experimental set-up.

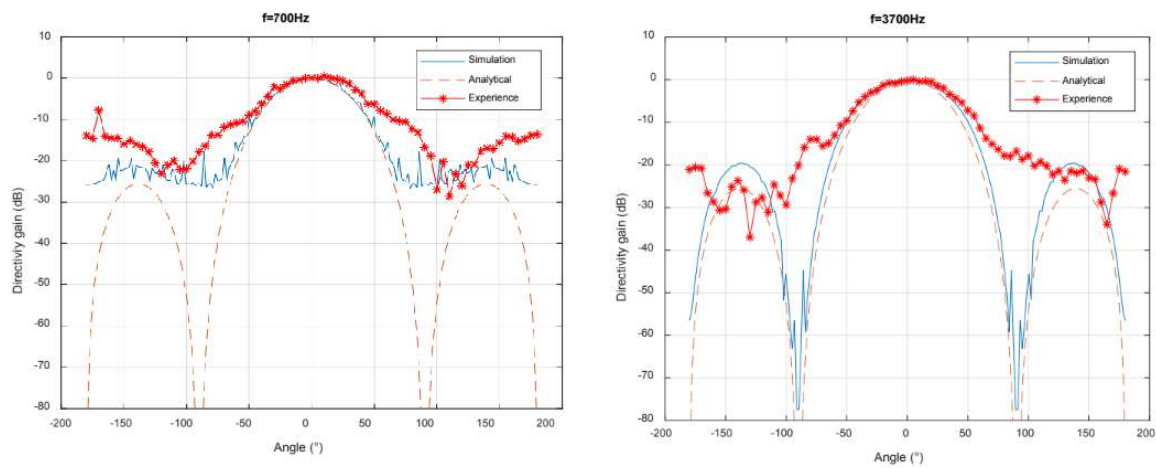


Figure 3: Angular response of the differential array at 700 Hz (left) and 3700 Hz (right).

acquisition is performed through a Heim front-end, from Zodiac. The post-processing is done with Head Artemis v10.1 and Matlab R2015.

All the microphones have been characterized in an waveguide coupler, in order to measure the phase difference between the sensors as a function of frequency. Indeed, even though such class-one sensors are very precise and robust in the time, and because of the chosen methodology based on the gradient approximation, a very accurate knowledge of the phase relation has to be obtained.

4. Results

In this part, a small selection of results are presented. All the simulations have been performed with an in-house developed code, based on the equations mentioned in the model section.

4.1 Constructed directivity

Figure 3 presents the analytical, simulation and experimental levels as function of the angle for two frequencies, 700 Hz and 3700 Hz.

Figure 4 presents the reconstruction of the array directivity based on the experimental data as the function of the frequency. The phase mismatches between the sensors are taken into account. The

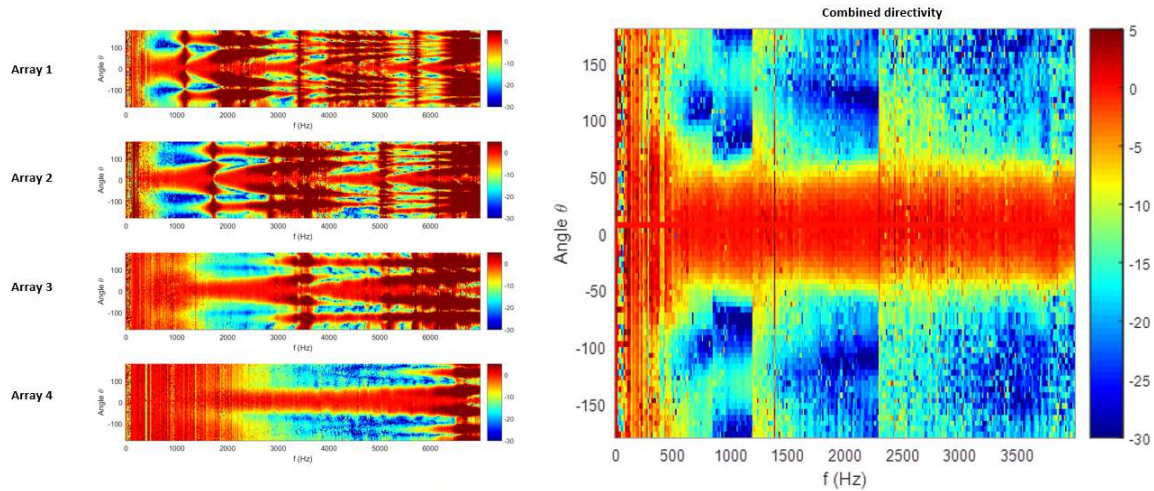


Figure 4: Reconstructed directivity from the experimental data as the function of the frequency.

response has been normalized by the array response at 0 degrees and it can be seen on figure 4 that the directivity of the array in the complete frequency range (200 Hz- 5000 Hz) is composed of four responses, associated to the four sub-arrays of the experimental set-up. The combined response displays an almost constant width of the main lobe in the [400 Hz - 5000 Hz] frequency range.

For each of these sub-arrays' responses, the WNG effect is observable in the lower frequencies bands, and results in a slight widening of the directivity. The frequency limit at which it is chosen to use a new sub-arrays response is determined as trade-off between this low frequency WNG effect and the spatial aliasing that can occur beyond a frequency depending on the microphone spacing.

4.2 1D localization of a noise source

The localization principle considered is based on the comparison between the omnidirectional response captured by any of the microphones of the array, and the response of this array. Knowing the directivity pattern of the antenna, the evaluation of the spectrum level difference between the omnidirectional response and the array response should allow the user to retrieve the angular incidence of the sound source.

Figure 5 shows a comparison between the omnidirectional noise spectrum and the array response for two different angles of arrival of the sound. The comparison at 0° shows almost no difference with the omnidirectional response in the spectrum induced by the array whereas at 30°, an effect on the noise spectrum is clearly visible and can be measured. The directivity diagram of the figure 4 can hence be used to link the measured level difference to the sound angle of arrival.

Several localization tests have been made for various angles of arrival. These tests are based on the experimental data gathered in the anechoic chamber with the rotating boom. For every localization test, the estimated angle of arrival is retrieved with an accuracy of $\pm 15^\circ$.

5. Discussion

5.1 Deviations between the analytical model and the experiment

From figure 3, it can be observed that the theoretical levels do not depend on the frequency, as they are the same in the two plots presented, which has been also observed for all the other frequencies not

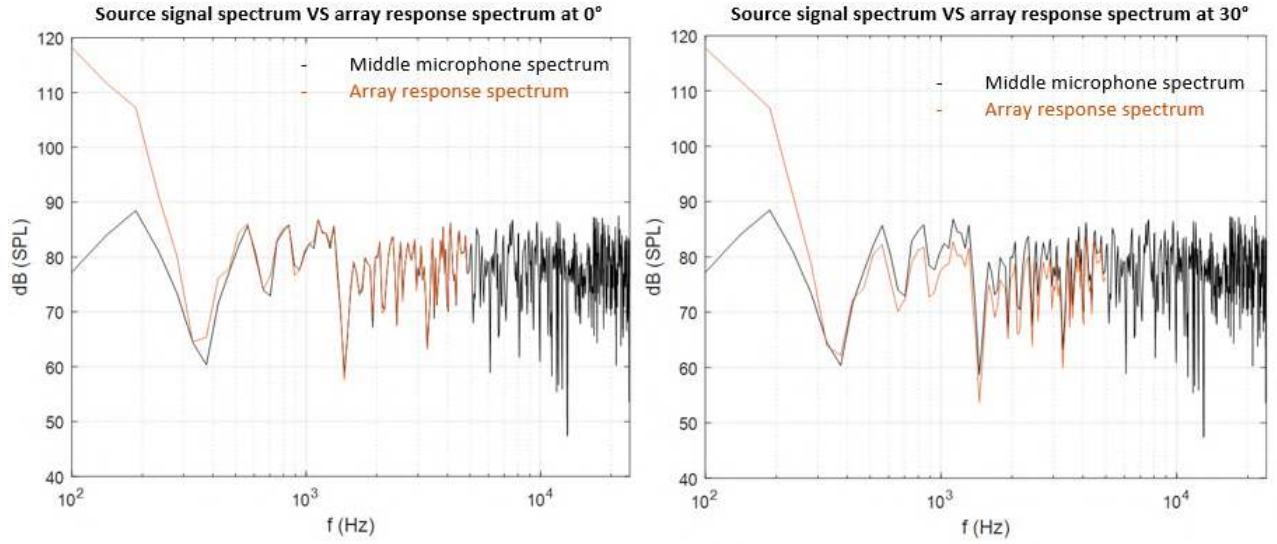


Figure 5: Array response at 0 (left) and 30 (right) degrees compared to omnidirectional response.

shown in this paper. However, both the simulations and the experimental results exhibit responses that depend on the frequency.

The first hypothesis that can explain these differences with regards to the analytical model is that the assumption of a plane wave propagation of the sound is not fully respected in the experimental set-up, given the short distances between the source and the microphones. Hence, the delay introduced in the post-processing treatment, and based on the hypothesis of a time propagation of plane waves, is not perfectly adapted to the delay of propagation of spherical waves between two microphones.

The second hypothesis that could explain the differences between the analytical model and the test results is the phase mismatch between the microphones, not taken into account in the analytical model. This leads to a higher residual background noise in the array response, especially at low frequencies, where the WNG phenomena is clearly visible.

5.2 Sound source localization

From these plots, and despite the differences observed between the models and the experimental results, it has to be observed that both the simulation and the experiment curves fit well with the theoretical prediction on the angular opening between $[-50^\circ; +50^\circ]$, with a good symmetrical shape.

The figure 4 shows that directivity is almost constant in the $[-50^\circ; +50^\circ]$ range over the whole frequency span. This result is in line with the theory and allows to use the created directional array for localization purposes.

As seen in the previous section, the angular accuracy reached with the experimental set-up is of $\pm 15^\circ$. This accuracy, obtained with one linear array is not yet good enough for actual localization purposes in an industrial context. To further improve the accuracy of the localization, a set up comprised of several linear differential arrays can be imagined. Placed at different locations in the area of investigation and with different orientations, the intersection of the localization results of each individual array should contribute to narrow down the area of the plausible sound source location.

6. Conclusion

The designed differential linear array presented in this paper, has been studied and characterized through analytical, numerical and experimental comparisons. The proposed fourth-order post-processing method, based on the theory of differential microphone arrays, has led to a directive array with a narrow asymmetrical response. The obtained directivity makes the array sensitive only to the sound coming from a given angular sector. Good agreement between the analytical model and the experimental directivity has been found and one dimensional localization tests with the designed array were conducted.

The localization accuracy reached with the designed differential array is not satisfying enough for direct use in noise source identification purposes within an aircraft but improvements of the array are possible and should contribute to better localization performances.

For instance, the WNG effect at low frequencies severely reduces the performance of the array in this range. An improvement of the phase matching between the microphones will contribute to a better behaviour. Furthermore, the first-order cardioid directivity is known to provide better performances with regard to the WNG at low frequencies. A cascading post-processing based only on cardioid weightings should result in a slightly wider directivity along the array direction, but with better low frequencies performances.

A method combining the results of several linear differential arrays can also be considered and is likely to improve the localization accuracy through the intersection of the results of each antenna. For such a set-up, with array placed looking at different directions in the area of investigation, a method for the geometrical and spatial calibration of the array network will be necessary. Methods based on cross-correlation and Time Of Arrival (TOA) or Time Difference Of Arrival (TDOA) estimations are possible approaches. These methods can use built-in controlled sound sources or ambient noise to spatially localize the array network in the referential of the zone of investigation ([4],[5]).

REFERENCES

1. J. Benesty and J. Chen, *Study and Design of Differential Microphone Arrays*, Springer Topics Signal Processing, (2013).
2. Ducourneau, J. and Planeau, V. and Nejade, A, *Design of a multipolar weighting for acoustic antennae*, Applied Acoustics (2009).
3. Huang, Chen, Benesty, *On the design of robust steerable frequency invariant beampatterns with cocentric circular microphone arrays*, ICASSP2018, (2018).
4. Brutti Alessio, *Distributed Microphone Networks for sound source localization in smart rooms*, DIT-University of Trento, (2007).
5. Aarabi Parham, *The fusion of distributed microphone arrays for sound localization*, EURASIP Journal on Advances in Signal Processing, (2003).